



## DEVELOPMENT OF ROOM IMPULSE RESPONSE PROCESSING SOFTWARE

**Maite Atín**

*Universidad Nacional de Tres de Febrero, Ingeniería de Sonido, Caseros, Buenos Aires,  
Argentina  
email: maiteatin@gmail.com*

**Alejandro Sosa Welford**

*Universidad Nacional de Tres de Febrero, Ingeniería de Sonido, Caseros, Buenos Aires,  
Argentina  
email: alejandrososawelford@gmail.com*

**Joaquín Ponferrada**

*Universidad Nacional de Tres de Febrero, Ingeniería de Sonido, Caseros, Buenos Aires,  
Argentina  
email: joacoponfe@gmail.com*

---

This document describes the development of a Python-based program designed to compute the acoustic parameters of a given room, from either an impulse response measurement, or a sine sweep measurement. Descriptions of both back-end and front-end code are presented. The GUI allows for different linearization techniques to be chosen in order to calculate the desired parameters. The obtained results are contrasted with the performance of two available commercial softwares. From a series of generated synthetic IR responses used to evaluate the developed code's performance, a valid operating bandwidth of 125 to 20,000 Hz is determined. Dispersion values for each type of linearization technique are also presented.



*Keywords: Room acoustic parameters, Python software*

---

## 1. Introduction

Room acoustics are very diverse. They depend on the size, materials and geometry of a room, and cause subjective impressions on the listeners based on reflections, sound decay, and interaural differences [1]. Many of these issues can be studied in room impulse response (RIR) analysis. The International Organization for Standardization (ISO) 3382 [2] establishes methods for obtaining indicators of acoustical properties in rooms such as reverberation time and clarity. Angelo Farina has developed advancements in impulse response measurements in noisy and non-linear systems by implementing sine sweep recordings [3].

The aim of this study is to obtain room acoustic parameters from a measurement with sine sweeps according to the ISO 3382, and acoustic parameters for binaural measurements ~~with a KEMAR (Knowles Electronic Manikin for Acoustic Research)~~. A graphical user interface (GUI) is developed in Python for the handling of impulse response measurement files, applying analysis procedures and obtaining results. The processing behind the GUI is realized in blocks to calculate  $T_{20}$ ,  $T_{30}$ , EDT,  $EDT_t$ ,  $C_{50}$ ,  $C_{80}$ , IACC,  $IACC_{early}$ ,  $T_t$  and for different user-selected options, including smoothing procedures, octave band or third-octave band analysis, and background noise compensation, all of which are detailed in the following sections.

## 2. Theoretical framework

The characteristics of a linear time invariant system, such as a room, can be fully described from its impulse response  $h(t)$ . This function can be obtained in different ways, such as a balloon pop, a gunshot, by interrupted noise method or with an MLS (Maximum-Length Sequence). However, real systems present nonlinearities which can influence the impulse response. Farina [3] has developed an alternative impulse response method employing a sine sweep that allows the separation of linear response from non-linear distortion.

Most of the room acoustical parameters can be obtained from RIR analysis, particularly on the energy time curve (ETC) and how its decay is. In a measurement of real room impulse responses, background noise affects the results. Therefore, finding the crossing point between the decay and background noise is necessary to implement the calculus.

For the monophonic RIR, reverberation time is obtained through  $T_{20}$ ,  $T_{30}$ , EDT, clarities are expressed as  $C_{50}$ ,  $C_{80}$  and centre time as  $T_s$  according to the ISO 3382 [2]. In the case of binaural RIR recording using a head and torso simulator (KEMAR), the IACC can also be computed, including its different forms depending on the time interval under analysis ( $IACC_{early}$ ,  $IACC_{late}$  and  $IACC_{all}$ ). For both types of measurements, transition time  $T_t$  and  $EDT_t$  are also calculated. The results are presented in octave bands or third octaves bands at the user's choice, as established by the IEC 61260 standard [4].

### 2.1 Energy Time Curve

The energy time curve represents the decay of the energy of an IR as a function of the time. On a logarithmic scale, an ideal RIR has a decay that is similar to a decreasing linear function, as shown in Figure 1.

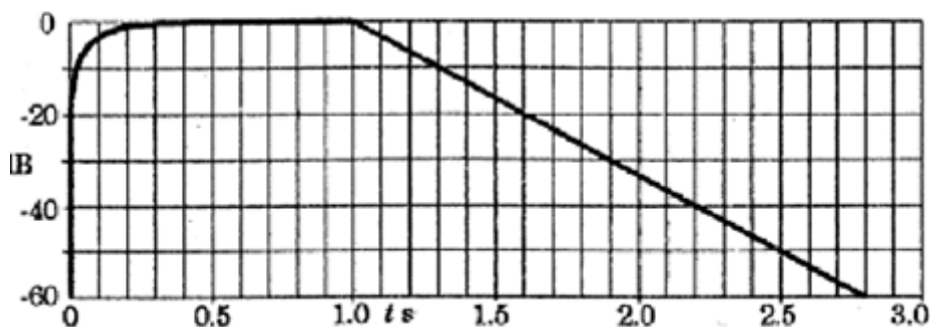


Figure 1. ETC of an ideal RIR in dB.

Even though a real RIR does not have a perfectly straight decay, its ETC can be found by smoothing the energy curve  $h^2(t)$  until it reaches into the background noise. In this work, two methods can be used to obtain the ETC of a RIR: Schroeder's inverse integral, or median moving filter.

Schroeder integration method [5] is implemented applying Eq. (1), where  $h^2(t)$  represents the energy curve, and  $T$  is the limit of the integral.

$$ETC(t) = 10 \log_{10} \left[ \frac{\int_t^T h^2(\tau) d\tau}{\int_0^T h^2(\tau) d\tau} \right] \quad (1)$$

The limit  $T$  represents the crossing between decay and background noise, and can be obtained by **Lundeby's method**. This procedure, ~~as described by Lundeby in his paper *Uncertainties of Measurements in Room Acoustics* [6]~~, consists of an iterative algorithm for estimating the background noise level and the late decay slope until a crosspoint between the two is found. This then becomes the point from which the reverse-time integration of the impulse response is performed.

Another noise compensation is Chu's method [7]. This is a method in which the root mean square value (RMS) of the background noise is subtracted from the RIR energy, before being integrated by Schroeder to find the ETC. It is assumed that the last 10% of the RIR is exclusively stationary background noise. With this correction, the integrated backward curve approximates the desired decay curve.

Schroeder's inverse integral also can be solved without compensation for background noise. In that case, the limit of the integral corresponds to the length of the RIR (theoretically, the integral is calculated up to infinity).

Instead of using Schroeder's method, the linearization of the decay can be performed by implementing a moving median filter (MMF). From a time window specified in milliseconds, the filter runs through the signal, replacing each sample with the median of its neighboring samples that are within the time window, i.e., the value that is midway between all the values of the window.

## 2.2 Fractional Octave Band Filters

The evaluation of room acoustic parameters is generally done by filtering the measured impulse response signal, as it is of interest to find the parameters corresponding to fractional octave bands. These fractional octave band filters are specified by the IEC 6120 standard [4], which details the nominal midband frequencies, the procedures for determining each band's upper and lower frequency and the filter's attenuation, among other parameters. It is important to note that the filtering methods applied are a key factor in the variability of the acoustic parameters that will be obtained, as explained by Huszty et al. [8]

Most commercially available room impulse response processing softwares (such as Aurora, developed by A. Farina) give the user the option to analyse the RIR, filtering either with octave bands or one-third octave bands.

As shown by Rasmussen et al. [11] for short reverberation times (between 0.1 and 0.2 s.), one-third-octave band analysis is prone to introduce high levels of ringing to the measurements. Rasmussen proposes a method which reduces the effect of the interference

in the filtered signals and consists of time-reversing the RIR, once before and then after the implementation of the filter. Time-reversed analysis has been shown to better approximate the results of posterior reverberation time calculations.

### 2.3 Parameters



#### 2.3.1 Reverberation Time

When the source of sound in a room is suddenly turned off, a certain time is required to elapse before all the sound energy is practically absorbed by the environment. The acoustic energy density in a room is associated with the sound after the first reflection [9].

The reverberation time (RT) is defined as the time, expressed in seconds, required for the sound pressure level to decrease by 60 dB. This is equivalent to one millionth of the energy after the cessation of a sound source. In order to do this measurement on an impulse response, a high signal to noise ratio (SNR) is required. In a real environment this is difficult to achieve, and for this reason EDT (Early Decay Time), T20 and T30 are defined [2]. These parameters allow the calculation of RT in a smaller dynamic range, with the corresponding extrapolation to the definition of reverberation time.

T20 corresponds to the decay line between -5 and -25 dB, whereas T30 corresponds to the interval from -5 to -35 dB. The early decay time (EDT) relates to the initial decay of the impulse response, between 0 and -10 dB. All these must be measured from the slope of the impulse response energy integrated by fractions of octave bands. This slope is obtained by a line fitted by least squares method in the indicated intervals.

#### 2.3.2 Clarity

The ISO 3382-1 standard [2] defines acoustic quantities related to the subjective perceptions of listeners. Among these is clarity ( $C_{80}$ ), a parameter expressed in decibels that expresses the ratio of the sound energy arriving between the first 80 ms and the rest of the response ("late-arriving energy"). A similar parameter known as  $C_{50}$  is practically identical except that the ratio is calculated for the first 50 ms of the sound energy. These parameters are supposed to give an overall impression of the intelligibility of speech (in the case of  $C_{50}$ ) or the clarity of music (in the case of  $C_{80}$ ). Eq. (2) shows the expression of the calculation determined in the ISO 3382-1.

$$C_T = 10 \log \left( \int_0^T p^2(t) dt / \int_T^\infty p^2(t) dt \right) \quad (2)$$

where T represents the limit of integration, being 50 milliseconds for  $C_{50}$  and 80 milliseconds for  $C_{80}$ .

#### 2.3.3 Interaural Cross Correlation

In the case of binaural recordings, measured for instance using a dummy head, the "spatial impression" of a room can be estimated through the interaural cross correlation coefficient

(IACC), although as the ISO 3382-1 standard notes, its use has not yet been widely accepted. Regardless, this parameter can be employed to give an approximate idea of the “spaciousness” of the room and how closely the left and right ear canal signals are correlated. The IACC is obtained by Eqs (3) and (4).

$$IACF(\tau) = \left[ \int_{t_1}^{t_2} p_L(t) \cdot p_R(t + \tau) dt \right] / \left[ \int_{t_1}^{t_2} p_L^2(t) dt \int_{t_1}^{t_2} p_R^2(t) dt \right] \quad (3)$$

$$IACC = \max | IACF(\tau) | \quad \text{for } -1 \text{ ms} < \tau < +1 \text{ ms} \quad (4)$$

where  $p_L(t)$  y  $p_R(t)$  represents the impulse response of the left and right channel respectively in a binaural RIR.

#### 2.3.4 Transition Time

The transition time ( $T_t$ ) is defined as the instant in which the cumulative energy of the impulse response reaches 99% of its total energy [10]. This parameter, in its objective form, determines the limit between the deterministic and stochastic regions of the impulse response.

#### 2.3.5 Center Time

The center time ( $T_s$ ) is defined by the ISO 3382-1 standard as the time corresponding to the center of gravity of the squared impulse response. This parameters alludes to the perceived balance of the room between clarity and reverberation [2]. Its calculation from the RIR is applied through Eq. (5).

$$T_s = \int_0^{\infty} t \cdot p^2(t) dt / \int_0^{\infty} p^2(t) dt \quad (5)$$



### 3. Development of software

An open source, standalone application written entirely in Python is developed for the purpose of processing room impulse response measurements and obtaining the acoustic parameters described above, with the added functionalities of visualizing the impulse response and its decay in a graph and exporting the results as a .CSV file. Its main functions consist of loading measurements and calculating the parameters according to the analysis options selected by the user. The source code is available on [GitHub](#) with some RIRs to perform evaluations.

### 3.1 Signal Flow

Figure 3 shows a flow chart that represents the possible routes of processing a room impulse response in the developed software. The intersection points of the arrows refer to processing points that can be decided by the user. The elements in curly brackets are also the user's choice, with default values established. The processing is divided into four main parts:

- 1) Obtaining the RIR: loading it from a .wav file, or generating it by the convolution between a recorded sine sweep and an inverse filter loaded or generated from the interface. Stereo RIR can be loaded here, all calculations and parameters will be performed for each channel, in addition to calculating their respective IACC values. 24-bit .wav files are supported, with variable sample rates. (Soundfile Python library is used for importing audio files.)
- 2) Fractional Octave Band Filters: based on the IEC 61260 standard (filter designed according to the specified base-2 rules). Frequency response of the 1/1 octave filter utilized is shown in Figure 2. (Instability can be seen at lower bands.) Filter order is set to 8. Time-reversed analysis is implemented at this stage reversing IR signal both before and after filtering.

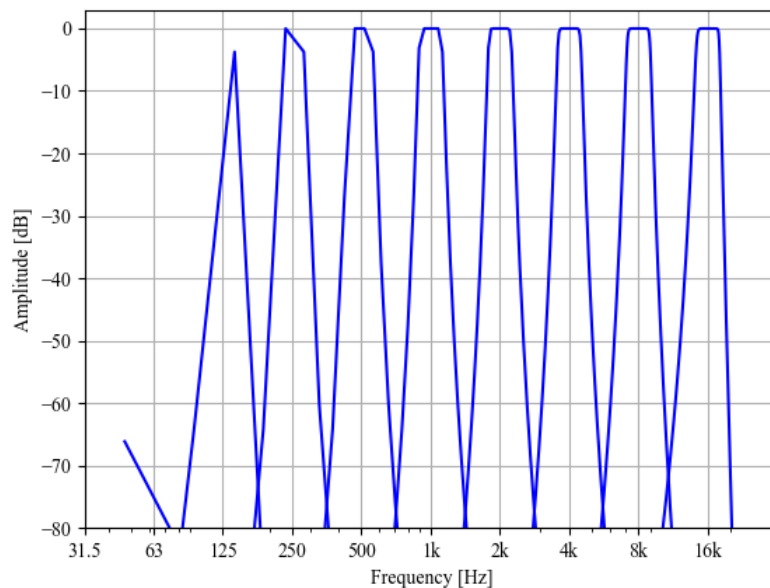


Figure 2. 1/1 Octave digital filter frequency response.

- 3) Smoothing: the RIR squared is linearized by Schroeder with Lundebay or Chu noise compensation, or without compensation; or linearized through a Moving Median Filter with a window length of the user's choice (50 ms by default, to guarantee correct analysis in the lower frequency of interest, 20 Hz). Smoothing of signal is performed for every frequency band of the filtered signal.
- 4) Obtaining acoustical parameters: Obtained from the smoothed impulse response as previously explained. Tt and EDTt parameters are obtained after discarding the information prior to the IR's first reflection. EDTt is calculated by performing the same linearization as the one used in step 3), chosen by the user.

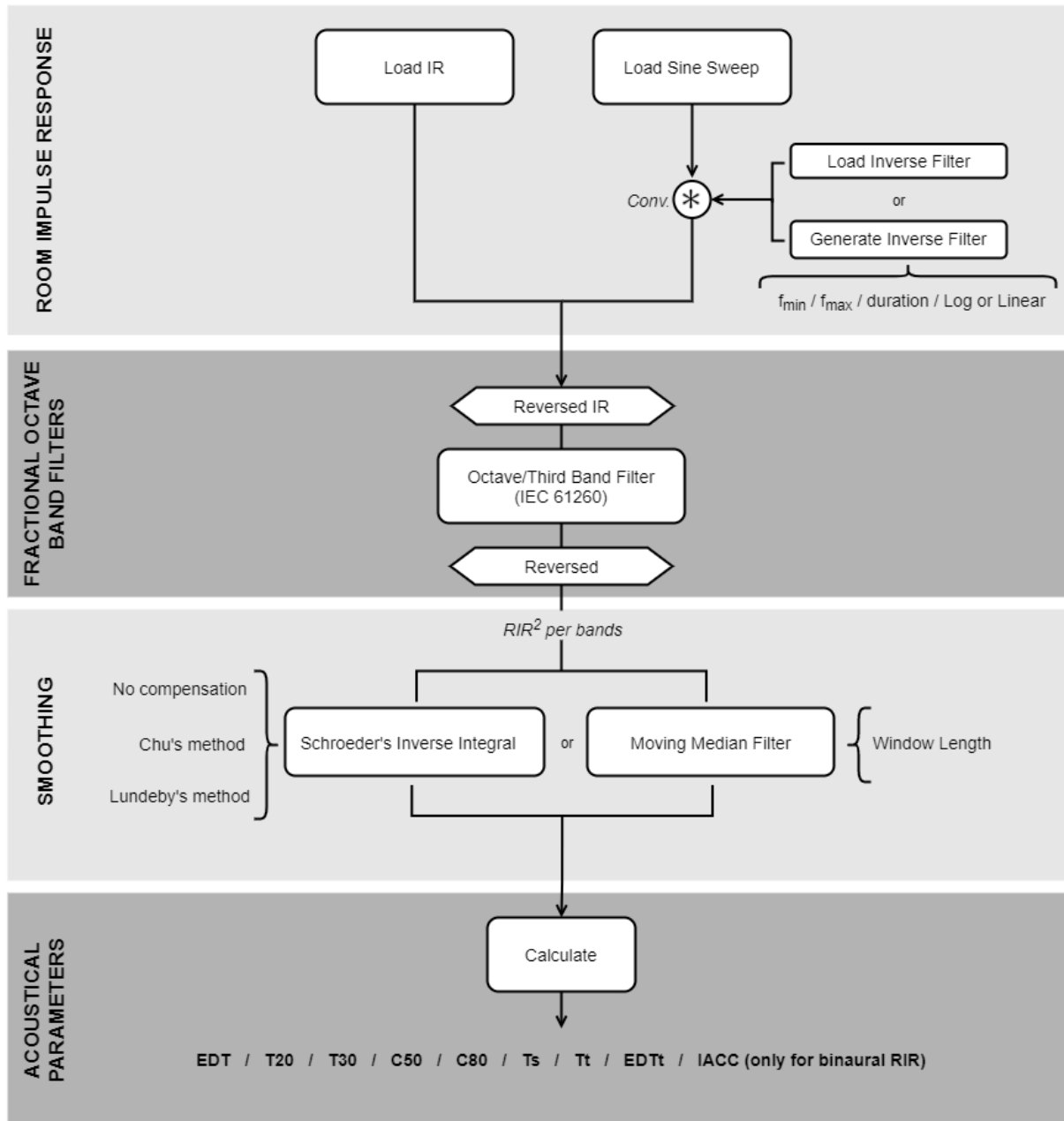


Figure 3. Signal flow of the developed software.



### 3.2 Graphical User Interface (GUI)

The goal is to create a software that is simple and efficient, with a clear and straightforward interface that is intuitive and user friendly. Figure 4 shows the main window of the application which opens upon startup. Its two main options appear as buttons at the top of the window, to give the user the option between loading an existing impulse response file or loading a sine sweep. The latter option takes the user to another window where they will be prompted to load a recorded sine sweep and (optionally) an inverse filter file.



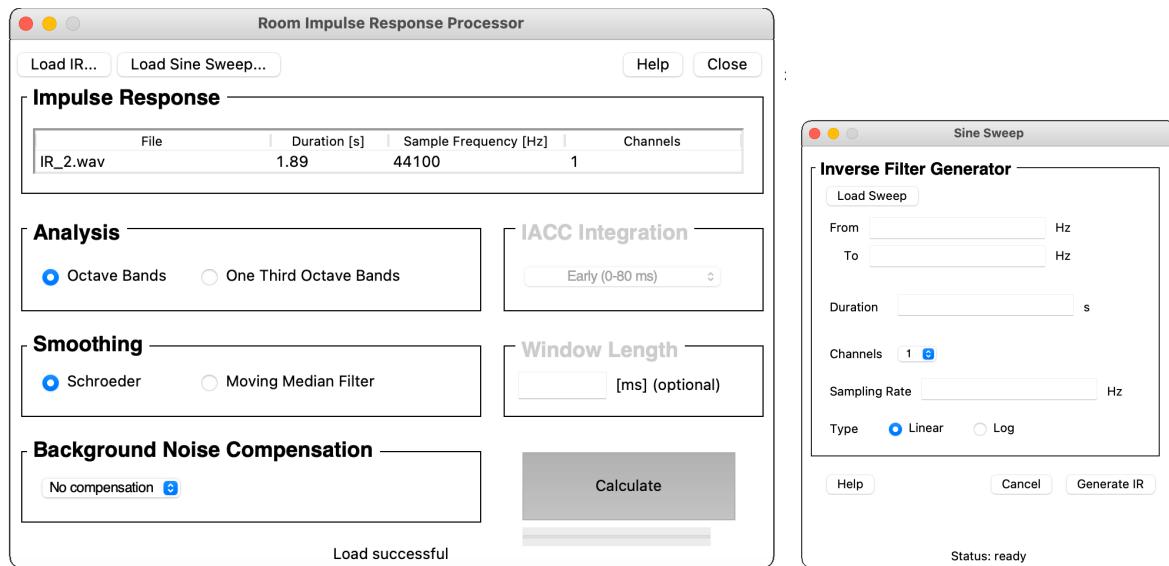


Figure 4. Main Window of the RIR Processing Application (Left). Sine Sweep Loading Window (Right).

Once a RIR file is loaded (whether directly or generated from a sine sweep), its information is displayed on the Impulse Response table so that the user can verify they have loaded the RIR that they wish to analyse. The following blocks are highlighted with emphasized labels that guide the user as they choose between filter analysis modes (octave bands or one-third octave bands), smoothing method, along with two options (Background Noise Compensation and Window Length) that enable and disable depending on whether the user has chosen Schroeder integration or Moving Median Filter as the Smoothing method.

Additionally, if the loaded RIR is binaural (i.e. consists of two channels) the user can select the IACC Integration to be displayed ( $IACC_{early}$ ,  $IACC_{late}$  and  $IACC_{all}$ ).

After hitting the “Calculate” button, the code runs through all the processing blocks and calculates the acoustic parameters which, once the process is completed, are displayed in a new window (Figure 5) alongside a graph including the impulse response for each frequency band, its corresponding decay curve and vertical lines indicating the positions of  $T_t$  and  $T_s$  (if applicable). The user can change the information that is displayed on the graph, by clicking on each frequency band on the table below it. If the RIR under analysis is binaural, the user can also select which channel (L or R) is represented on the parameters table and on the graph. Results can be exported to a .csv file.



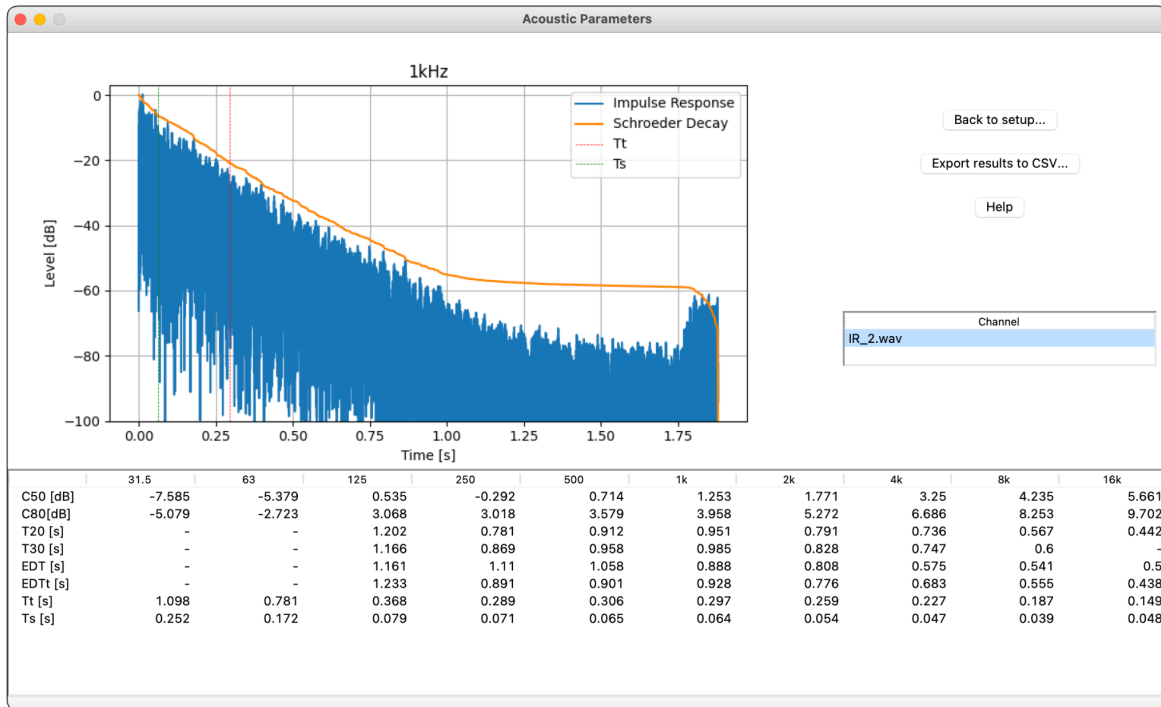


Figure 5. Acoustic Parameters Window.

### 3.3 Error control

Each parameter's calculated value is evaluated to avoid reporting spurious results. Said results can be the product of a number of different issues, which can range from outliers in the measurement still present after the smoothing of the signal or insufficient S/N ratio in the analyzed frequency band (which could occur if analysis is performed over frequencies where the original IR signal didn't have any information). Furthermore, invalid arguments given by a user in the main window of the GUI will result in a warning message dialog box informing the user on how to correct their inputs.



## 4. Results

Once the software's initial development process is completed, a performance analysis is carried out. This is done in two ways: 1) comparing it against other processing software; 2) processing synthetic RIRs. These processes are detailed in the following subsections.

### 4.1 Comparison with other processing softwares

The comparison of the code developed in this work (called RIRPA from now on, whose acronym stands for *Room Impulse Response Processing Application*), is made against Aurora [12] (developed by Angelo Farina) and a code developed by Densil Cabrera in MATLAB [13]. RIRPA is evaluated for different smoothings, either by Schroeder or Moving Median Filter. In the case of Schroeder, the three noise compensation options (Chu, Lundeby, without compensation) are compared. For MMF, a window of 50 ms is used.

A set of RIRs are processed in the three softwares (Aurora, Densil Cabrera and RIRPA). The results of T20 calculations of a RIR corresponding to the Apollo theater, located in Buenos Aires city, are presented below. Appendix A shows the results of the comparison for two more real RIRs, and for synthetic RIRs with different characteristics.

Figure 6 shows the T20 calculation results in octave bands for each software. It can be seen that above 125 Hz, all processing softwares give practically the same results. This is not the case for 63 and 31.5 Hz bands, where Aurora gives a high T20 value, while Densil Cabrera and RIRPA do not give results due to the control of unreasonable values (except in Schroeder without compensation).

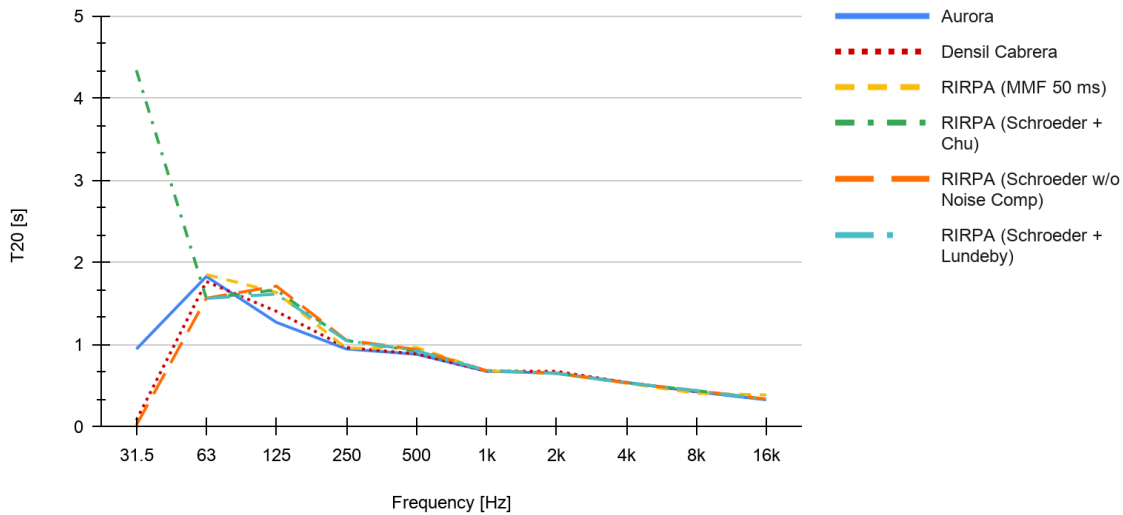


Figure 6. Comparison of T20 values.

For the EDT, the comparison of the results is similar to the T20. In the 125 Hz band, dispersion in the values are detectable. This dispersion of the RIRPA results is also observed in the comparison of T30 even with greater notoriety, especially for the Schroeder process without noise compensation (i.e. without truncating the inverse integral), and for the MMF process.

The difference is more noticeable in T30 since the analysis interval is greater and the linearization of the IR is more affected by the noise. For Schroeder + Lundebay compensation, the result is very close to that given by Aurora and Densil Cabrera. Therefore, the differences mentioned above, are related to the lack of noise compensation, or insufficient compensation. This can be verified in Appendix A.

For  $C_{50}$  clarity (Figure 7), the results tend to have the same type of deviation as mentioned above. Up to 125 Hz, the variation between the results is around 6 dB. Below 125 Hz the results show too much variability, thus they are not reliable.

The same relationship is seen in  $C_{80}$  clarity (Appendix A), with a 6 dB dispersion among all compared softwares above 125 Hz.

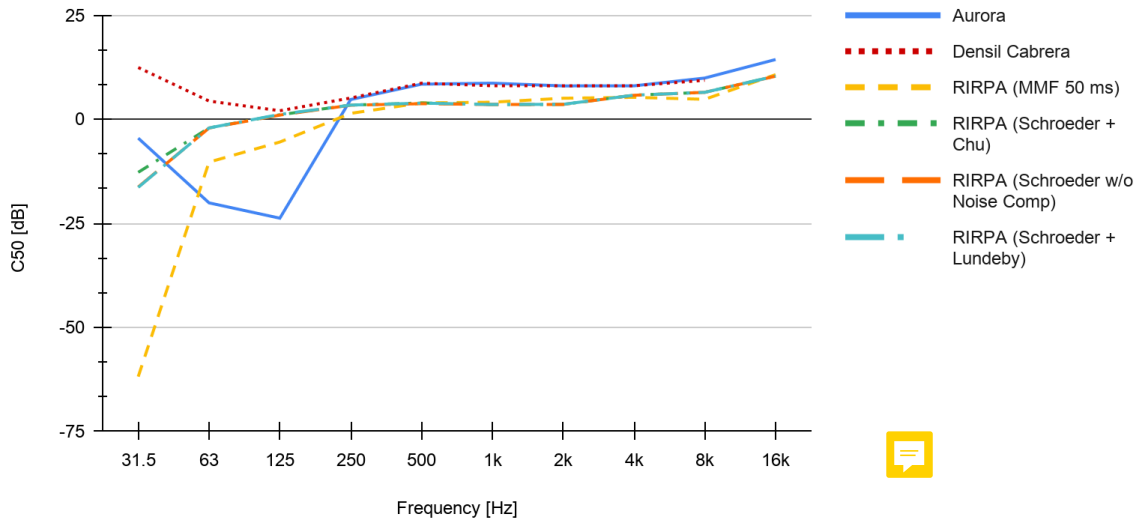


Figure 7. Comparison of C50 values.

For the center time, again the dispersion appears in the low frequency bands (Figure 8). Between 125 Hz and 16 kHz, the variability is less than 0.2 seconds, with Aurora's results being the farthest from the rest.

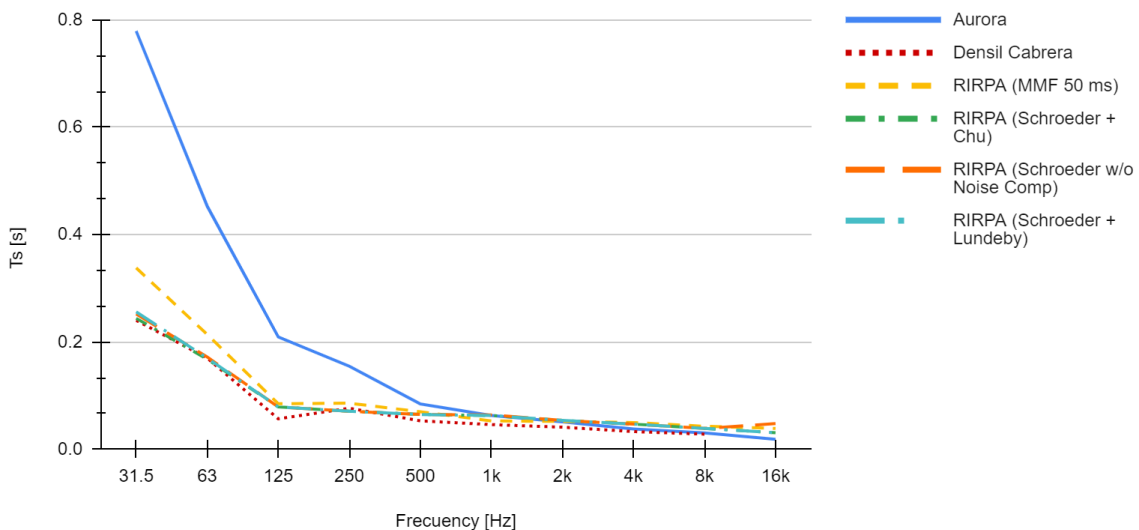


Figure 8. Comparison of  $T_s$  values.

Comparisons of the transition time ( $T_t$ ) and early decay transition time ( $EDT_t$ ) are not carried out, since neither Densil Cabrera nor Aurora perform this calculation.

For IACC parameters, the comparison was performed in a similar manner as with the other parameters, this time utilizing a generic stereo IR. Results can be seen in figure 9. Since no smoothing is performed on the analyzed signals, only one set of results from RIRPA's analysis is plotted, giving the 3 sets of curves shown below. There are noticeable differences between the results obtained from all three softwares when comparing from 125 Hz to 16 kHz bands. It is of note that even if results vary greatly, there's a tendency of IACC reducing its value, as frequency increases, which makes theoretical sense.

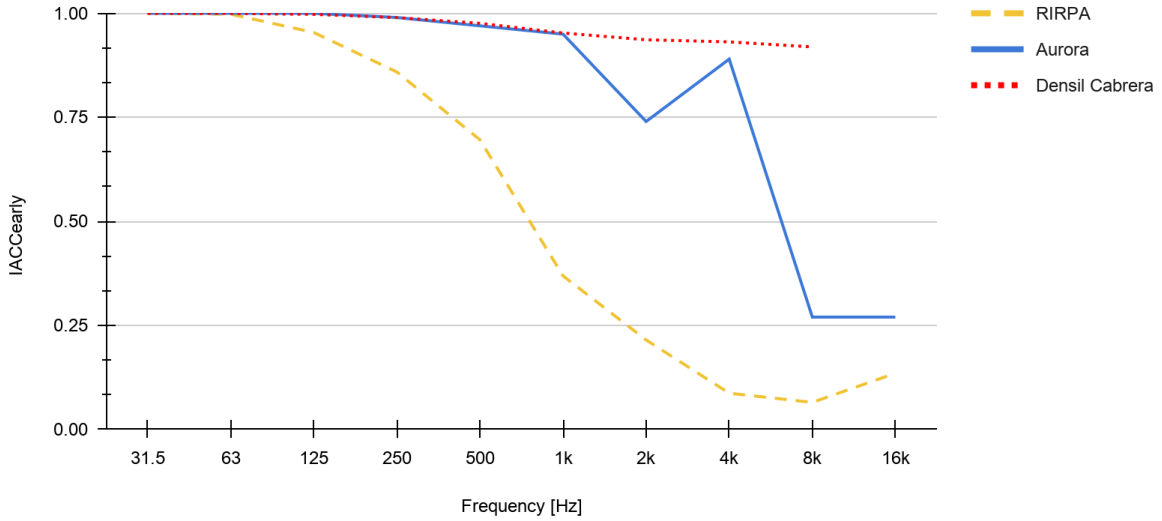


Figure 9. Comparison of IACC-early values.

## 4.2 Processing synthetic RIRs

A generator of synthetic RIRs with Gaussian noise is made in order to validate the results of the RIRPA processing. Through these RIRs it is possible to control the reverberation time in the synthesis of these signals, as expressed in Eq. (6).

$$y(t) = A \cdot e^{-b \cdot t} \cdot n(t) + M \cdot n(t) \quad (6)$$

where  $n(t)$  represents Gaussian noise, with an amplitude of  $M$  for the representation of background noise.  $A$  indicates the initial amplitude of the impulse, and  $b$  the decay rate subsequently related to the reverberation time as indicated by Eq. (7). The values of  $A$  and  $M$  are established to have an impulse-to-noise ratio (INR) [14] greater than 35 dB in order to obtain the calculation of  $T_{30}$ , following Eq. (8)

$$RT = \frac{3}{b \cdot \log e} \quad (7)$$

$$INR = L_{impulse} - L_{noise} \quad (8)$$

Synthetic signals were also used to study Lundeby processing to find the truncation time of the Schroeder integral, this being the crosspoint between the energy decay and the background noise. For the synthetic RIRs this is given by Eq. (9)

$$t_c = -\frac{1}{b} \ln\left(\frac{M}{A}\right) \quad (9)$$



Next, in Figure 10, the calculation comparison of  $T_{20}$  for the same softwares mentioned in the previous subsection is shown. The analysis is carried out for a synthetic RIR with 0.3 seconds of reverberation time in all its bands. In the graph, it can be seen that below 125 Hz the calculation is far from what was expected, as inferred from the previous section.

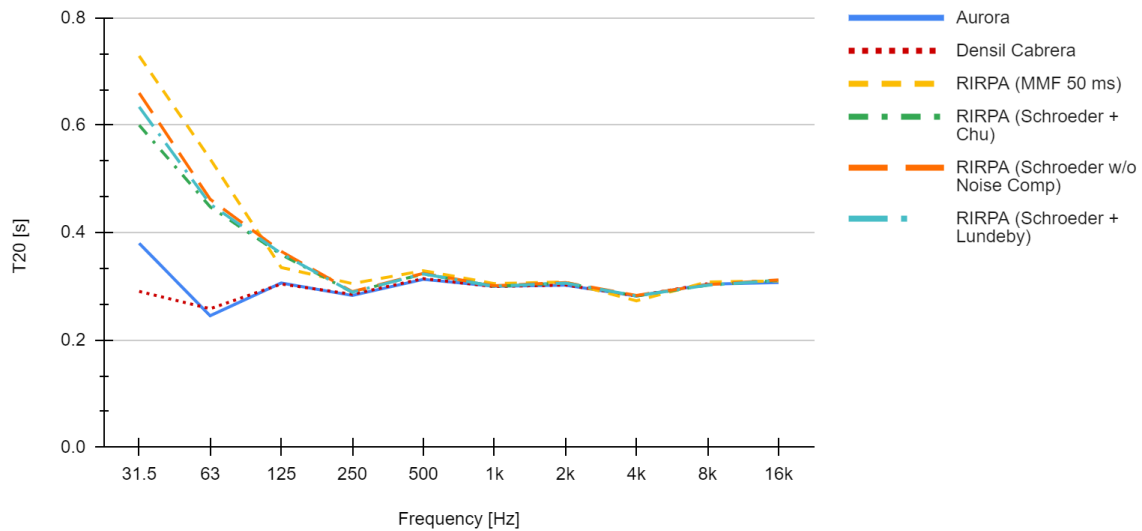


Figure 10. Comparison of T20 values.

### 4.3 Conflict sources and Troubleshooting

For the analyzed results, the biggest dispersions compared to the commercial softwares are present in the lowest octave bands. In some cases this could be attributed to lack of information or insufficient S/N ratio required to properly analyze said intervals, however, across all calculations, the implemented band-pass filters generate considerable instabilities as shown in figure 2, for the lowest bands. Due to this, most of the results obtained for the frequencies below 125 Hz are usually to be discarded. (Note that, even when comparing the results of the commercial softwares, big differences are to be found in some cases, meaning that for some measurements, “accurate” values of acoustic parameters are just not possible to report with a high degree of certainty.)

This, in addition to the analysis of Sections 4.1 and 4.2, determines the validity bandwidth of the developed software between 125 Hz and 20 kHz.

A possible solution to this problem is implementing a different filter, with an improved low frequency response. This is sometimes performed by performing downsampling techniques in the lower frequency bands. The effect of the time-reversed analysis proposed by Rasmussen et al. is also hard to quantify, given that results of calculations performed on signals with short reverberation time are hindered by the same low frequency filter problems, as discussed in this section.

### 4.4 Dispersion of results analysis

For the determined bandwidth (125 Hz - 20 kHz), the results obtained from synthetic IRs are analyzed, where the exposed parameters are controlled from the synthesis explained above (Eqs. (6) through (9)). Three impulse responses are used, one with low RT (0.3 s in all bands), one with mid RT (1 s in all bands), and one with high RT (3 s in all bands). The results obtained in the processing are analyzed to quantify the dispersion between RIRPA's and the expected values from the synthesis of the signals. Table 1 reports the largest dispersions observed in the specified bandwidth for each IR, with the different processing methods offered. The calculated values for each frequency band are found in Appendix B.

Table 1. Dispersion of results for the three different synthetic IRs under analysis.

0.3 s						
	EDT [s]	T20 [s]	T30 [s]	C50 [dB]	C80 [dB]	Ts [s]
MMF (50ms)	$0.30 \pm 0.11$	$0.30 \pm 0.04$	$0.30 \pm 0.04$	$3.4 \pm 5.7$	$7.3 \pm 8.4$	$0.04 \pm 0.02$
Schroeder no comp.	$0.30 \pm 0.09$	$0.30 \pm 0.07$	$0.30 \pm 0.07$	$3.4 \pm 6.9$	$7.3 \pm 8.9$	$0.04 \pm 0.02$
Schroeder w/ Chu	$0.30 \pm 0.09$	$0.30 \pm 0.06$	$0.30 \pm 0.04$	$3.4 \pm 6.9$	$7.3 \pm 9.1$	$0.04 \pm 0.02$
Schroeder w/ Lundeby	$0.30 \pm 0.09$	$0.30 \pm 0.06$	$0.30 \pm 0.05$	$3.4 \pm 6.9$	$7.3 \pm 9.1$	$0.04 \pm 0.02$
1 s						
	EDT [s]	T20 [s]	T30 [s]	C50 [dB]	C80 [dB]	Ts [s]
MMF (50ms)	$1.00 \pm 0.41$	$1.00 \pm 0.07$	$1.00 \pm 0.17$	$-3.8 \pm 6.9$	$-1.3 \pm 4.7$	$0.14 \pm 0.07$
Schroeder no comp.	$1.00 \pm 0.14$	$1.00 \pm 0.10$	$1.00 \pm 0.11$	$-3.8 \pm 4.3$	$-1.3 \pm 4.7$	$0.14 \pm 0.07$
Schroeder w/ Chu	$1.00 \pm 0.14$	$1.00 \pm 0.10$	$1.00 \pm 0.10$	$-3.8 \pm 4.3$	$-1.3 \pm 4.7$	$0.14 \pm 0.07$
Schroeder w/ Lundeby	$1.00 \pm 0.07$	$1.00 \pm 0.10$	$1.00 \pm 0.14$	$-3.8 \pm 4.3$	$-1.3 \pm 4.7$	$0.14 \pm 0.07$
3 s						
	EDT [s]	T20 [s]	T30 [s]	C50 [dB]	C80 [dB]	Ts [s]
MMF (50ms)	$3.00 \pm 0.65$	$3.00 \pm 0.78$	$3.00 \pm 0.25$	$-9.1 \pm 4.9$	$-6.9 \pm 3.9$	$0.43 \pm 0.22$
Schroeder no comp.	$3.00 \pm 0.60$	$3.00 \pm 0.14$	$3.00 \pm 0.16$	$-9.1 \pm 3.6$	$-6.9 \pm 3.8$	$0.43 \pm 0.22$
Schroeder w/ Chu	$3.00 \pm 0.60$	$3.00 \pm 0.14$	$3.00 \pm 0.14$	$-9.1 \pm 3.6$	$-6.9 \pm 3.8$	$0.43 \pm 0.22$
Schroeder w/ Lundeby	$3.00 \pm 0.60$	$3.00 \pm 0.14$	$3.00 \pm 0.15$	$-9.1 \pm 3.6$	$-6.9 \pm 3.8$	$0.43 \pm 0.22$

From the results obtained, the moving median filter (MMF) processing presents the highest dispersion (for a time window of 50 ms), compared to the other methods. This analysis could be expanded considering windows of different durations.

The deviation obtained in the clarities is of considerable order. This is also true when evaluating the results of both Densil Cabrera software and Aurora.

For Ts, errors remain constant, regardless of the method, since the IR is processed prior to smoothing. The error in this case is due to the signal filtering stage. Tt and EDTt computed values weren't evaluated with the synthetic signals, since it wasn't possible to determine a theoretical correct value of these parameters from which to estimate the dispersion in RIRPA's results.

## **5. Conclusions**

The objective of developing a software for the calculation of acoustical parameters was achieved. The results obtained in the specified valid bandwidth are consistent with Aurora by Angelo Farina and Densil Cabrera's model. The limitations in low frequencies, due to the performance of the fractional octave filter, represent a possible future improvement which would allow the software to expand the range of reliability of its results.

The development is a software prototype, therefore the times of computations and internal processes do not have a high level of optimization. This point can also be improved.

For a second version of the software, it is also proposed to have greater options for the user, such as allowing the possibility to choose the frequency range of representation, which would reduce the computation time in case of requiring a fewer number of bands than the standard, and avoid results that are not consistent. It would also be beneficial to expand upon the validation of the results, including some way to analyse EDTt and Tt parameters.

## **6. References**

- [1] L. Beranek. Concert Halls and Opera Houses. 2nd edition. Springer (2002).
- [2] ISO 3382. Acoustics - Measurement of room acoustic parameters. International Organization for Standardization (2009).
- [3] A. Farina. Advancements in impulse response measurements by sine sweeps. Audio Engineering Society, Vienna (2007).
- [4] IEC 61260. Electroacoustics - Octave-band and fractional-octave-band filters. International Electrotechnical Commission (2004).
- [5] M. R. Schroeder. New method of measuring reverberation time. Acoustic Society of America (1964).
- [6] A. Lundeby, T. E. Vigran, H. Bietz, and M. Vorländer, "Uncertainties of Measurements in Room Acoustics," *Acustica*, vol. 81 (1995).
- [7] W. T. Chu. Comparison of reverberation measurement using Schroeder's impulse method and decay-curve averaging method. *Journal of Acoustical Society of America* (1978).
- [8] C. Huszty, N. Bukuli, A. Torma and F. Augusztinovicz. Effects of filtering of room impulse responses on room acoustics parameters by using different filter structures. Budapest University of Technology and Economics, BME Dept. of Telecommunications, Budapest, Hungary (2008).
- [9] R. F. Barron. Industrial Noise Control and Acoustics. Marcel Dekker, Inc. (2003).



- [10] A. Bidondo, L. Shtrepi, L. Pepino, A. Astolfi. Analysis of the room acoustic texture parameters in function of diffusers location and distribution inside a small concert hall. Proceedings of the International Symposium on Room Acoustics (2019).
- [11] B. Rasmussen, J. H. Rindel, H. Henriksen. Design and Measurement of Short Reverberation Times at Low Frequencies in Talks Studios. Journal of the Audio Engineering Society, 39(1/2), 47-57. (1991)
- [12] Aurora Pulg-ins. Online: [http://pcfarina.eng.unipr.it/Aurora\\_XP/index.htm](http://pcfarina.eng.unipr.it/Aurora_XP/index.htm)
- [13] D. Cabrera, J. Xun, M. Guski. Calculating Reverberation Time from Impulse Response: A Comparison of Software Implementation. Australian Acoustic Society (2016).

## Appendix A

The RIR under analysis is represented in Figure A1. Figures A2 through A7 show the comparison in octave bands of calculations between Aurora, Densil Cabrera and RIRPA for different processing conditions, for the EDT, T20, T30, C50, C80 and Ts parameters. More RIRs processing comparisons, including analysis in one-third octave bands, are available [online](#).

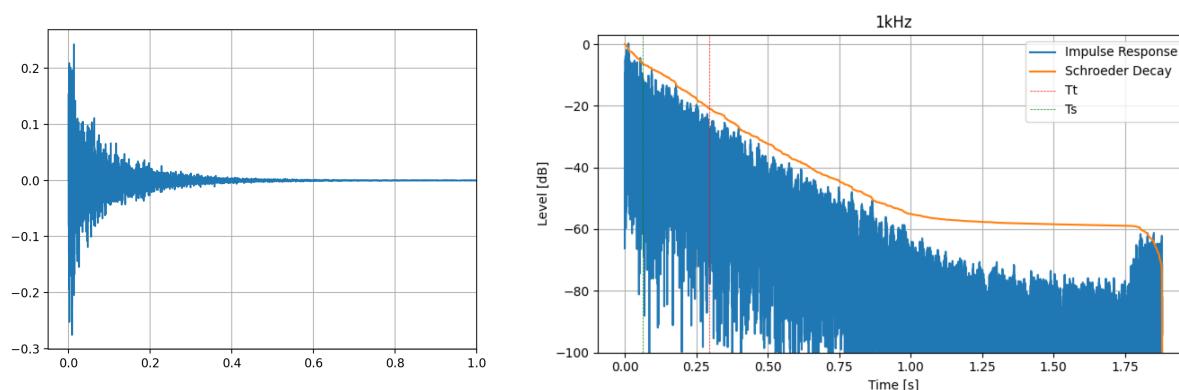


Figure A1. Impulse response waveform (left) and its level and decay as analyzed for 1 kHz octave band in RIRPA (right).

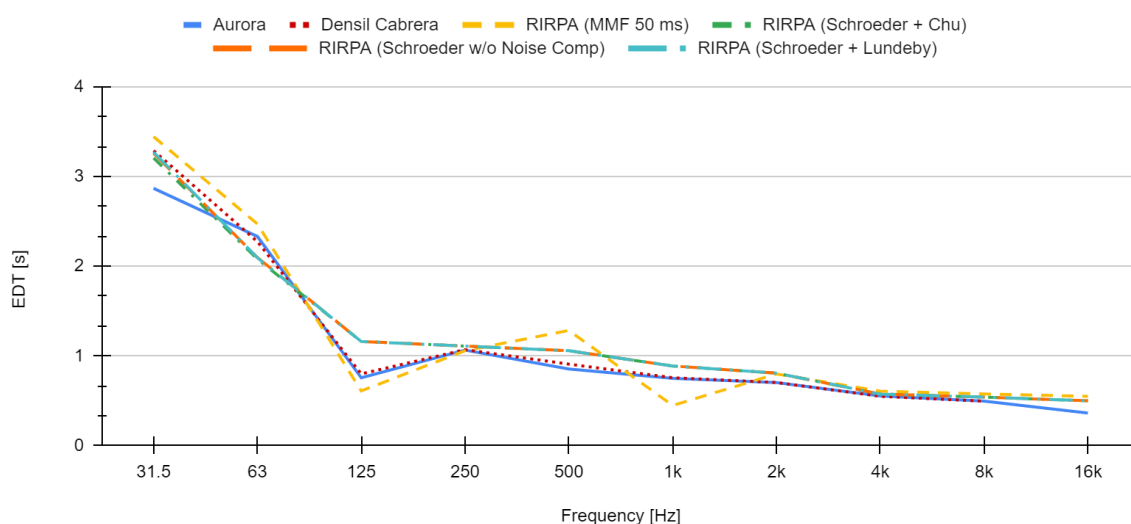


Figure A2. EDT values for octave bands. Comparison between softwares and for different smoothing and noise compensation configurations in RIRPA.

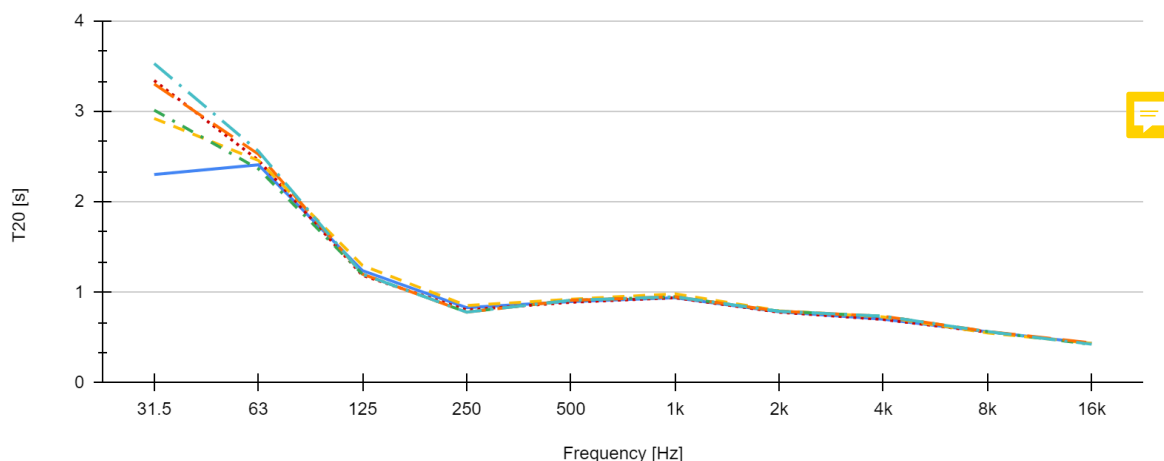


Figure A3. T20 values for octave bands. Comparison between softwares and for different smoothing and noise compensation configurations in RIRPA.

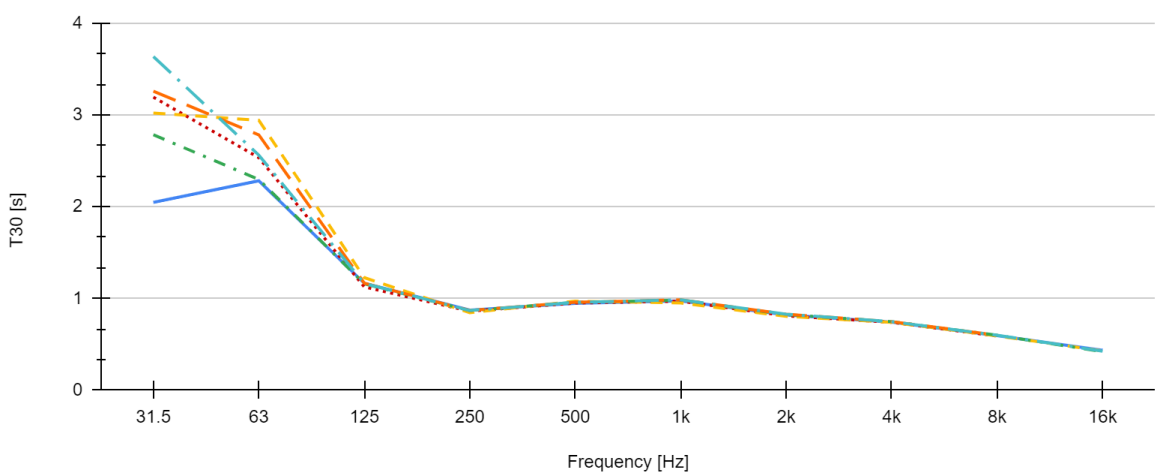


Figure A4. T30 values for octave bands. Comparison between softwares and for different smoothing and noise compensation configurations in RIRPA.

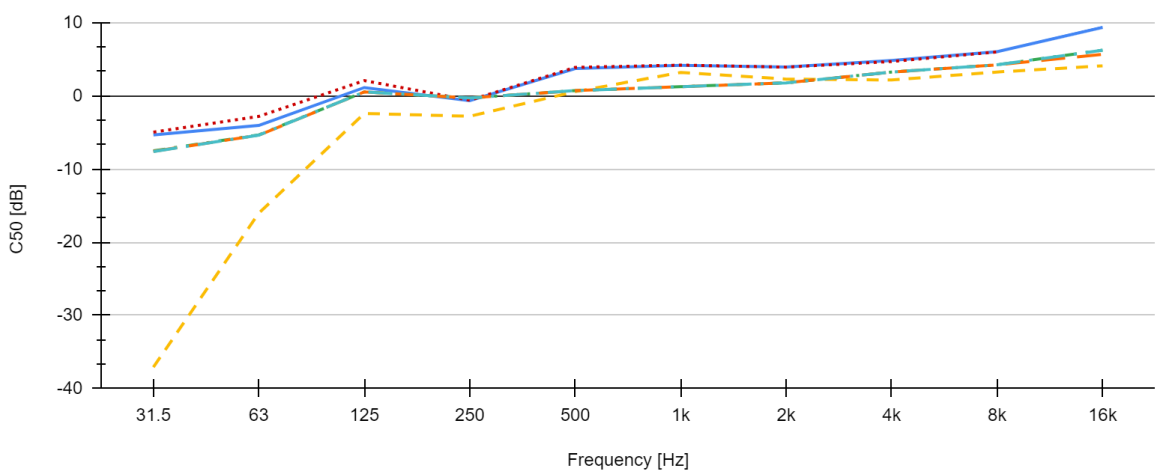


Figure A5. C50 values for octave bands. Comparison between softwares and for different smoothing and noise compensation configurations in RIRPA.

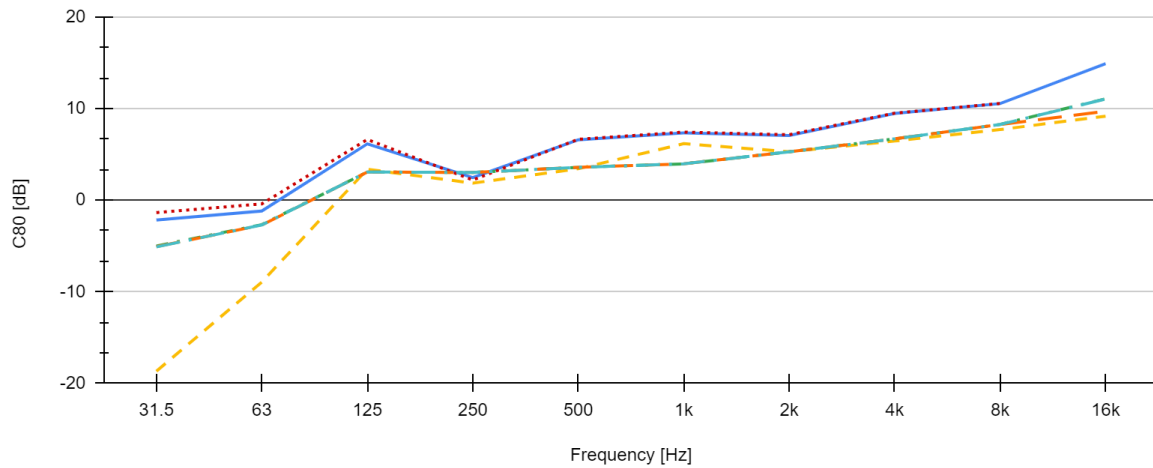


Figure A6. C80 values for octave bands. Comparison between softwares and for different smoothing and noise compensation configurations in RIRPA.

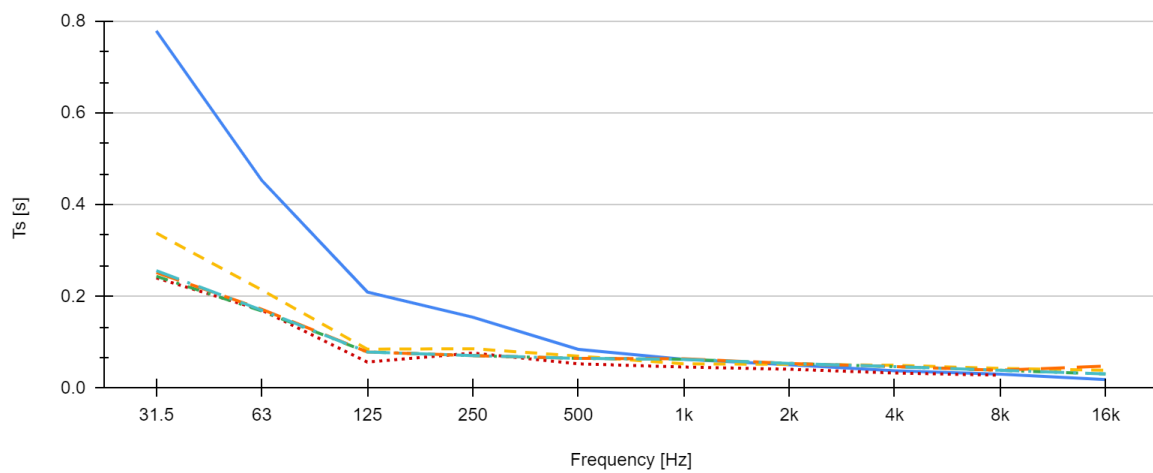


Figure A7. Ts values for octave bands. Comparison between softwares and for different smoothing and noise compensation configurations in RIRPA.



## Appendix B

Calculated parameters in RIRPA for synthetic IR with  $RT = 1$  s, octave band analysis using different smoothing configurations. 31.5 and 63 Hz bands are excluded from analysis for reasons detailed in Section 4.4.

Table B1. Moving Median Filter, Window Length = 50 ms.

	125 Hz	250 Hz	500 Hz	1 kHz	2 kHz	4 kHz	8 kHz	16 kHz
C50 [dB]	-10.8	0.0	-0.4	-0.2	-0.2	-0.2	0.1	-0.4
C80 [dB]	-4.9	3.1	2.3	2.5	3.4	2.9	3.2	2.7
T20 [s]	0.97	1.08	0.98	1.06	1.05	1.02	1.05	1.00
T30 [s]	0.96	1.17	1.02	1.05	1.02	1.01	1.04	1.01
EDT [s]	0.84	1.11	1.41	1.13	0.90	1.02	0.97	1.02
Ts [s]	0.12	0.08	0.07	0.08	0.07	0.07	0.07	0.08

Table B2. Schroeder, no Background Noise Compensation.

	125 Hz	250 Hz	500 Hz	1 kHz	2 kHz	4 kHz	8 kHz	16 kHz
C50 [dB]	-1.8	0.5	0.2	-0.1	0.3	0.0	-0.2	-0.2
C80 [dB]	1.8	3.1	3.3	3.1	3.4	3.1	2.8	2.9
T20 [s]	0.96	1.10	1.04	1.01	1.05	1.02	1.02	1.02
T30 [s]	1.11	1.11	1.04	1.03	1.04	1.03	1.04	1.04
EDT [s]	0.86	0.99	1.01	0.99	0.95	0.97	1.04	1.02
Ts [s]	0.08	0.07	0.07	0.07	0.07	0.07	0.08	0.07

Table B3. Schroeder + Lundeby Compensation.

	125 Hz	250 Hz	500 Hz	1 kHz	2 kHz	4 kHz	8 kHz	16 kHz
C50 [dB]	-1.8	0.5	0.2	-0.1	0.3	0.0	-0.2	-0.1
C80 [dB]	1.8	3.1	3.3	3.1	3.4	3.1	2.8	2.9
T20 [s]	0.96	1.10	1.03	1.01	1.05	1.02	1.02	1.02
T30 [s]	1.09	1.10	1.03	1.03	1.04	1.02	1.03	1.03
EDT [s]	0.86	0.99	1.01	0.99	0.95	0.97	1.04	1.02
Ts [s]	0.08	0.07	0.07	0.07	0.07	0.07	0.08	0.07

Table B4. Schroeder + Chu Compensation.

	125 Hz	250 Hz	500 Hz	1 kHz	2 kHz	4 kHz	8 kHz	16 kHz
C50 [dB]	-1.8	0.5	0.2	-0.1	0.3	0.0	-0.2	-0.1
C80 [dB]	1.8	3.1	3.3	3.1	3.4	3.1	2.8	2.9
T20 [s]	0.95	1.10	1.03	1.01	1.05	1.02	1.02	1.02
T30 [s]	1.07	1.10	1.03	1.02	1.04	1.02	1.03	1.03
EDT [s]	0.86	0.98	1.01	0.99	0.95	0.97	1.04	1.02
Ts [s]	0.08	0.07	0.07	0.07	0.07	0.07	0.08	0.07